The FHP-MP model as multiparticle Lattice–Gas

Yu. Medvedev

Abstract. An extension to the Lattice–Gas Boolean models up to integer values of the particle velocity vectors is proposed. A new FHP-MP model is featured. Experiments on simulation of a fluid using the new model were carried out. The comparison with the known results is made.

1. Introduction

One of the promising directions of the physical processes simulation is that with cellular automata. Cellular-automaton models of flows called the Lattice–Gas were proposed in the seventies of the last century [1] and since then are promptly advanced. These models are discrete; their ground is the Boolean algebra. It allows one to construct efficient programs and to minimize the computer costs.

But simplicity of the Lattice–Gas superimposes some limitations on the area of their application. Here are some of them: the superior limit of the Reynolds number amounts some hundreds; the boundary conditions allow setting only the immovable walls; the simulation of a transonic velocity is usually accompanied by distorting results. In this paper, an attempt is undertaken to solve these problems and to propose a new kind of the Lattice–Gas model, which is called the FHP-MP (multiparticle) cellular automaton. It is a generalization of the classic FHP (Frish, Hasslacher, Pomeau) model on Boolean vectors [2]. In the new model, more than one particle in a cell with equal velocity vectors can be present. Attempts to use particles of miscellaneous mass in the Lattice–Gas were undertaken [3], but by different reasons they were not gaining acceptance.

In this paper, the new FHP-MP model is featured, and results of its experimental research are given, such as two-dimensional approximation of a flow between two planes, a flow with a flat valve and a flow of a circular obstacle. In these examples, a correlation in a corresponding variety of a flow velocity and the flow pressure rate between the FHP-MP and the FHP-I models is demonstrated. A poiseuille flow for the new model is obtained. Swirls were obtained, and the Kármán vortex street is visible in the presence of a valve or a circular obstacle, this showing to the possibility of the simulation of turbulent properties of a flow.

2. Specification of the FHP-MP model

2.1. The basic definitions. As a cellular automaton, the FHP-MP model is denoted by a triplet (W, A, N), where $W = \{w_1, w_2, \ldots\}$ is a set of *cells* allocated in corresponding sites in some discrete space. Each cell $w \in W$ is associated with a finite state machine (FSM) A called *the elementary FSM*. Its states are given by an integer-valued vector, as distinct from a Boolean vector in the classic FHP model. Each cell $w \in W$ is correlated with some coordinates $x(w)$ and $y(w)$ on the Cartesian plane. Therefore, between any two cells $w_1 \in W$ and $w_2 \in W$ it is possible to easily calculate a distance $d(w_1, w_2)$.

For each cell $w \in W$ an ordered set $N(w) = \{N_i(w) : N_0(w) = w, N_i(w) \in W \wedge d(w, N_i(w)) = 1, i = 1, 2, \ldots, b\}$ is determined. Its terms belong to *a neighborhood* with the cell w and are called its *neighboring cells* or *neighbors*. The constant b characterizes the number of non-identical neighbors of each cell $w \in W$. Cells are neighbors to themselves. There is a correspondence between the elementary automaton A outputs in a cell $w \in W$ and the inputs of neighbors of this cell and vice versa. Thus, the structure of the cellular automaton cells set W is a graph in which vertexes are cells, and edges from the set are the neighborhood relation. This graph has a regular lattice and degree of its vertices equal to b. The cell state is represented by a vector with integer-valued components. A set of states $s(w)$ of all cells $w \in W$ at the same instant t is called *a global state* $\sigma(t) = \{s(w_1), s(w_2), \ldots\}$ of the cellular automaton.
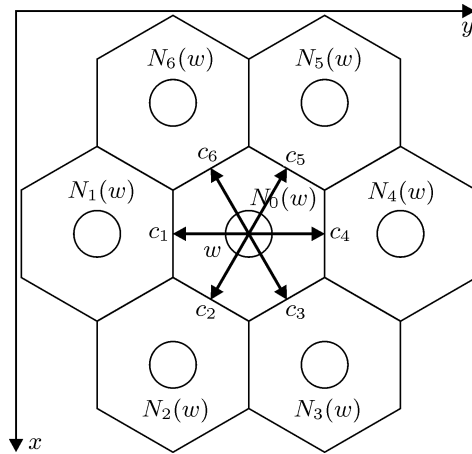

Figure 1. Velocity vectors of particles and numbering of neighbors

2.2. The neighbourhood relation. Each cell in the classic FHP model has six neighbors ($b = 6$). In some modifications of the model, each cell is as well a neighbor to itself (possibly several times), that stipulates the possibility of the presence of the rest particles. The ground of the FHP-MP model is the FHP model with one rest particle. In Figure 1, the cell w, and its neighbors $N_i(w)$, $i = 0, 1, \ldots, 6$, are represented. Thus, the number of neighbors of each cell w of the FHP-MP model is equal to seven, one of the neighbors is the cell w, i.e., $N_0(w) = w$.

Unlike the FHP, in the FHP-MP model, the components $s_0(w)$, $s_1(w)$, ..., $s_6(w)$ of a state vector $\boldsymbol{s}(w)$ are not Boolean, but integer. Thus, the mass of particles in a cell w is equal to:

$$m(w) = \sum_{i=0}^{b} s_i(w), \tag{1}$$

where $b = 6$ is the number of possible directions of a velocity vector, s_i is the ith component of the states vector $\boldsymbol{s}$. The physical interpretation of the vector $\boldsymbol{s}(w)$ components values is the following: s_i defines the number of unit mass particles, whose velocity vectors $\boldsymbol{c}_i$ are directed towards the neighbors $N_i(w)$.

The model momentum $\boldsymbol{p}$ in a cell $w \in W$ is the total of all momenta directed to all neighbors $N_i(w)$, where $i = 0, 1, \ldots, b$, and $b = 6$:

$$\boldsymbol{p}(w) = \sum_{i=1}^{b} s_i(w)\boldsymbol{c}_i(w). \tag{2}$$

From (1), with allowance for Figure 1, it is easy to compute the total momentum $\boldsymbol{p}$ of the projections p_x and p_y onto the Cartesian axes Ox and Oy:

$$p_x = \frac{\sqrt{3}}{2}(s_2 + s_3 - s_5 - s_6), \tag{3}$$

$$p_y = s_4 - s_1 + \frac{1}{2}(s_3 + s_5 - s_2 - s_6), \tag{4}$$

where s_i is the sum of velocity vectors of all particles in a cell w directed to the neighbor $N_i(w)$.

2.3. The behavior of the cellular automaton. We introduce three types of cells $w \in W$. The *conventional cells* $w_c \in W_c$ we will call those, in which both the mass and momentum conservation laws are satisfied. *The wall cells* $w_w \in W_w$ are the cells, in which the mass conservation law is satisfied, but the momentum conservation law can be violated. And, finally, *the source cells* $w_s \in W_s$ are cells, in which both the law of mass conservation, and the law of momentum conservation can be violated. Sets of conventional cells W_c, of walls W_w, and of sources W_s do not intersect pairwise ($W_c \cap W_w = \emptyset$, $W_c \cap W_s = \emptyset$, $W_w \cap W_s = \emptyset$). Integration of these sets coincides with a set of all cells of the automaton ($W_c \cup W_w \cup W_s = W$). The behavior of walls and sources specifies the boundary conditions of the cellular automaton.

In the FHP-MP model, the cellular automaton with a synchronous operation is used. In each cycle, there is a replacement of states $\boldsymbol{s}(t)$ in all cells, by the states $\boldsymbol{s}(t + 1) = \delta(\boldsymbol{s}(t))$, where $\delta(\boldsymbol{s}(t))$ is a next-state function

of the elementary FSM A. The cellular automaton thus changes its global state $\sigma(t)$ to a new global state $\sigma(t+1)$.

Each cycle of the cellular automaton processing has two phases: *propagation* and *collision*. So, a next-state function of the elementary FSM consists of a composition of the propagation function δ_1 and the collision function δ_2:

$$\delta(\boldsymbol{s}) = \delta_2(\delta_1(\boldsymbol{s})). \tag{5}$$

Each of the functions δ_1 and δ_2 should satisfy the laws of conservation of mass

$$\sum_{w \in W} \sum_{i=0}^{b} \delta_j(s_i(w)) = \sum_{w \in W} \sum_{i=0}^{b} s_i(w), \quad j \in \{1,2\}, \tag{6}$$

and momentum

$$\sum_{w \in W} \sum_{i=0}^{b} \delta_j(s_i(w)\boldsymbol{c}_i(w)) = \sum_{w \in W} \sum_{i=0}^{b} s_i(w)\boldsymbol{c}_i(w), \quad j \in \{1,2\}. \tag{7}$$

According to the fluid flow dynamics, the presence of these two phases is interpreted as follows. Collisions implement diffusion in fluids, and propagation implements the matter transport process in a flow. Further, these two phases are explicitly featured.

Propagation phase. In the propagation phase, in each cell $w \in W$ each particle specified by the components $s_i(w)$, at $i = 1, \ldots, 6$, propagates to the neighboring cell $N_i(w)$ corresponding to its velocity vector $\boldsymbol{c}_i$. The rest particles corresponding to s_0, remain in the cell w. Thus, the i-th component $s_i(w)$ of the state vector $\boldsymbol{s}(w)$ of the cell w after propagation adopts the value

$$\delta_1(s_i(w)) = \begin{cases} s_i(N_{((i+2) \bmod 6)+1}(w)), & \text{for } i = 1, 2, \ldots, b; \\ s_i(w), & \text{for } i = 0. \end{cases} \tag{8}$$

In spite of the fact that when propagating mass and momentum of particles in a single cell change, within the whole cellular automaton they are maintained, i.e., requirements (6) and (7) are fulfilled.

Collision phase. In the collision phase, there is a veering of particles velocity vectors directions according to some collision rules which are independent of states of the neighboring cells, i.e., δ_2 depends only on the state of its own elementary FSM. In the FHP-MP model, the function δ_2 is probabilistic. The collision rules for the above all types of the cells (conventional cells, walls, and sources) are as follows:

In the conventional cells $w_\mathrm{c} \in W_\mathrm{c}$, the function δ_2 is selected from such ones that the mass $m(w)$ and the momentum $\boldsymbol{p}(w)$ of particles in a cell were conserved:

$$\sum_{i=0}^{b} \delta_2(s_i(w_\mathrm{c})) = \sum_{i=0}^{b} s_i(w_\mathrm{c}), \quad \forall w_\mathrm{c} \in W, \tag{9}$$

$$\sum_{i=0}^{b} \delta_2(\boldsymbol{c}_i(w_\mathrm{c})) = \sum_{l=0}^{b} s_i(w_\mathrm{c})\boldsymbol{c}_i(w_\mathrm{c}), \quad \forall w_\mathrm{c} \in W. \tag{10}$$

One of the possible value obeying (9) and (10) should be chosen with equal probability. Fulfillment of (9) and (10) implies that of (6) and (7).

In the cells $w_\mathrm{w} \in W_\mathrm{w}$, which are walls, particles are "mirrored" backwards, thus violating the momentum conservation law:

$$\delta_2(s_i(w_\mathrm{w})) = \begin{cases} s_{((i+2) \bmod 6)+1}(w_\mathrm{w}), & \text{for } i = 1, 2, \ldots, b; \\ s_i(w_\mathrm{w}), & \text{for } i = 0. \end{cases} \tag{11}$$

Since the number of particles in a cell is not changing, requirements (9) and, therefore, (6) are satisfied. This is not so for (7), because directions of the velocity vectors $\boldsymbol{c}$ of the particles are changing, but this is admitted by the boundary conditions. Such a behavior of particles in wall cells simulates the requirement of zero speed of the flow on borders of obstacles.

Each cell-source $w_\mathrm{s} \in W_\mathrm{s}$ sustains the given concentration of particles $n_0(w_\mathrm{s})$. For this purpose, it generates particles with every possible direction of the velocity vector in case that the current concentration of particles $n(w_\mathrm{s}) < n_0(w_\mathrm{s})$. The number of generated particles is equal to a difference between a given concentration and a current one $n_0(w_\mathrm{s}) - n(w_\mathrm{s})$. It is possible to construct various obstacles by source cells. For example, having placed them in one line (usually, they are skirting a cellular array), we can obtain a source of a steady particle flow with a given concentration. A single source cell simulates an injector. Naturally, when generating new particles neither the mass $m(w_\mathrm{s})$ nor the momentum $\boldsymbol{p}(w_\mathrm{s})$ are conserved. The boundary conditions in cells-sources enable a breach of conditions (6) and (7).

Averaged values. In the simulation of flows, *microlevel* parameters of the cellular automaton such as a mass $m(w)$ and velocity of particles $\boldsymbol{c}_i(w)$ in each cell $w \in W$ do not have a practical significance. But *the averaged values* of their velocities $\langle \boldsymbol{u} \rangle$ and concentrations $\langle n \rangle$ over some *averaging vicinity* $Av(w)$, in which one includes all cells $w_j \in W$ placed not farther from a cell w, than at a certain distance r called *the averaging radius* are worth while. An averaged velocity is the total of velocity vectors of all particles in the averaging vicinity $Av(w)$, divided by the cardinal number of the averaging vicinity:

$$\langle u \rangle(w) = \frac{1}{|Av(w)|} \sum_{w_j \in Av(w)} \sum_{i=0}^{b} s_i \boldsymbol{c}_i, \tag{12}$$

where $|Av(w)|$ is the number of the cells situated in $Av(w)$, $\boldsymbol{c}_i$ is the unit velocity vector corresponding to the i-th digit of the state vector $\boldsymbol{s}(w_j)$, and s_i is a magnitude of the i-th digit of the state vector $\boldsymbol{s}(w_j)$ of the cell $w_j \in Av(w)$.

The averaged concentration of particles $\langle n \rangle$ is evaluated in the same vicinity $Av(w)$ as follows:

$$\langle n \rangle(w) = \frac{1}{|Av(w)|} \sum_{w_j \in Av(w)} \sum_{i=0}^{b} s_i. \tag{13}$$

Averaged values of velocity and concentration of particles are called the model velocity and the model pressure. They correspond to values of velocity and pressure of a simulated fluid and are *macrolevel* arguments.

We will note that average values of the model velocity and the model concentration will match with their physical analogs only in the case when the averaging vicinity $Av(w)$ consists exclusively of conventional cells $w_{\mathrm{w}} \in W_{\mathrm{w}}$. Otherwise, we will figure the values $\langle \boldsymbol{u} \rangle$ and $\langle n \rangle$ as indefinite. This requirement does not allow calculating the values $\langle \boldsymbol{u} \rangle$ and $\langle n \rangle$ for the cells, which are closer from walls and sources than averaging radius r.

3. Experimental study of the FHP-MP model

For validation of the proposed model, its program has been implemented. This allows carrying out computing experiments both on single-processor computers, and on multiprocessor and multicomputer systems. The code has been written in C, parallelism is implemented by means of the MPI library. The computing experiments performed with the FHP-MP model are described below. The qualitative behavior of a simulated flow is obtained.

3.1. Two-dimensional approximating of a fluid flow between two parallel planes. This experiment, which has already become a classical one, allows checking out a model onto correspondence with physics. Its essence is in the fact that the longitudinal flow velocity (the flow moves the lengthways Oy in a positive direction) with the velocity on the boundaries $\langle \boldsymbol{u} \rangle_b = 0$ should be proportional along the direction Ox under the parabolic law. The cellular automaton used in this computing experiment measures 100 by 2000 cells (along Cartesian axes Ox and Oy accordingly). The cells with coordinates in the interval $[(2,1),(99,1)]$ are sources. The cells with coordinates in spacing $[(1,1),(1,2000)]$ and $[(100,1),(100,2000)]$ are walls. Remaining ones are conventional cells. This 2D-construction is a cutting of a parallelepiped of the infinite width (lengthwise axis Oz) and it is an approximation of a three-dimensional flow between two parallel planes.
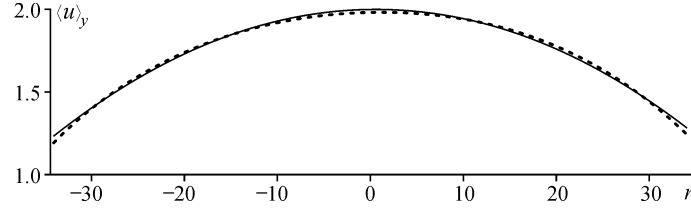
Figure 2. Poiseuille parabola and the experimental flow velocity

The projection of the flow velocity $\langle \boldsymbol{u} \rangle_y$ onto the axis Oy in a flow cross-section (lengthways Ox) is shown in Figure 2. The dotted curve illustrates the numerical simulation results. It is approximated by the parabola equation (in Figure 2, it is a solid curve):

$$\langle u \rangle_y(r) = -0.0008r^2 + 2, \qquad (14)$$

where r is a spacing interval between the middle of the bisecting point and an observed point of the cross-section.

The curve (14) is an inferential Poiseuille parabola; it is one of a few analytical solutions of the Navier–Stokes equation looking like:

$$\langle u \rangle_y(r) = \frac{dP}{4\eta l}(R^2 - r^2), \qquad (15)$$

where dP is a pressure drop on a part of a pipe in the length l, η is a dynamic viscosity of fluid, R is a pipe radius (in a two-dimensional case, it is a spacing interval between planes).

The number of iterations, after which one average is spent, is $T = 20000$. The averaging radius is $r = 15$ cells. According to the constraints imposed on (12) and (13), averaged values cannot be obtained in cells closer to walls than $r = 15$ cells. Therefore, idealized and experimental curves over the range, shown in the picture, are not declined to zero point.

A maximum velocity of the flow in the carried out experiment (Figure 2) was obtained equal to two; that is a little greater than in the classical FHP model. But it is not a maximum velocity; in the proposed multiparticle model it is possible to increase the concentration provided by sources, thus obtaining the flow velocity considerably superior the obtained one.

Results of this experiment demonstrate that the FHP-MP model correctly reproduces processes in a flow and corresponds to physics.

3.2. A flow with a valve. The following computing experiment has been carried out aimed at studying flows with obstacles. For this purpose, an additional boundary condition as a valve-shaped obstacle was added to the cellular automaton, being in the previous experiment. The valve has been placed at a distance to the source line equal to the third part of the pipe
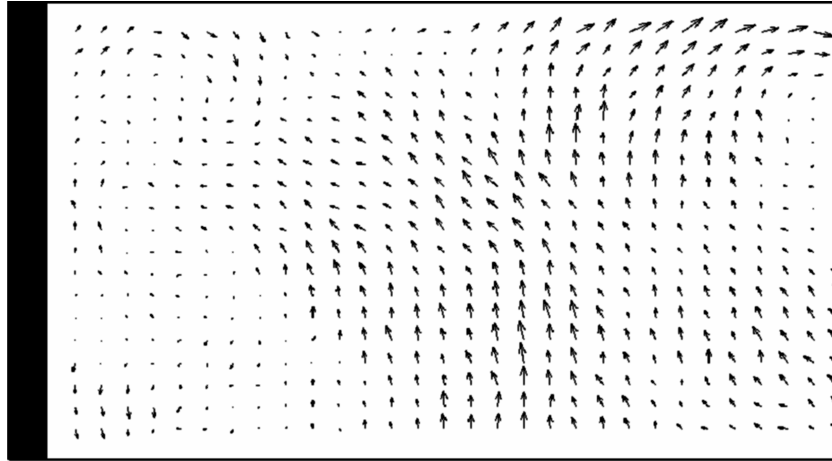
Figure 3. The flow velocity field with a valve as an obstacle.
A fragment behind the valve

length perpendicular to the flow propagation direction and has partitioned the pipe by half. The obtained velocity field resembles a streamline of the valve by the flow. The fact is, at the small-sized image scale encompassing the whole cellular automaton, high-velocity parts of the flow are only visible. It is necessary to discern a low velocity such as velocity behind the valve. In Figure 3, a fragment of the automaton, which is directly behind the valve, is given in a larger scale. The direction of each arrow in the figure coincides with a streamline in its basis, and its length is proportional to a flow velocity in that point. The flow is directed from left to right, the valve is figured in the left-hand side of the figure. On the painted fragment, flow vortices are clearly visible.
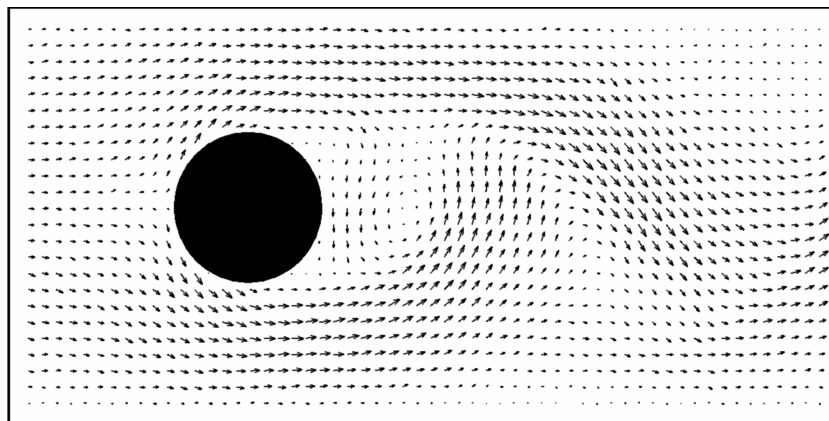

Figure 4. The flow velocity field with a circular obstacle

3.3. Streamlining of a circular obstacle. One more experiment has been carried out with a circular obstacle. It also demonstrates flow vortices. In the initial cellular automaton, a circle-shaped obstacle was added. The obtained velocity field of this automaton is shown in Figure 4. Behind the obstacle, an eddy is fetched away and the "S-turn" is visible. This "S-turn" is obviously alternative to the Kármán vortex street for a sufficiently small spacing interval to the skirting of the flow planes.

4. Conclusion

In this paper, the new cellular-automaton flow FHP-MP model, in which more than one particle are enabled in a cell with equal velocity vectors is proposed. The computing experiments have been carried out with this model; they demonstrate a correlation of the new model with the classic FHP model and with the physical laws. Experimentally, the obtained velocity field matches with the Poiseuille parabola. A maximum flow velocity in the experiments is slightly greater than that in the FHP model. In the new model, it is possible to augment the initial concentration of particles to obtain the flow velocity considerably exceeding that of the classic model. Therefore, we hope that the FHP-MP model will allow the simulation of a turbulent flow. The experiments with a valve and a circle-shaped obstacle convince us in this, because the flows with whirls were obtained, and the Kármán vortex street behind the obstacle is distinct.

References

[1] Hardy J., Pomeau Y., de Pazzis O. 2D lattice–gas model // J. Math. Phys.—1973.—No. 14.—P. 1746.

[2] Frisch U., Hasslacher B., Pomeau Y. Lattice–gas automata for Navier–Stokes equations // Phys. Rev. Lett.—1986.—No. 56.—P. 1505.

[3] Rothman D. H., Zaleski S. Lattice–Gas Cellular Automata: Simple Models of Complex Hydrodynamics.—Cambridge University Press, 1997.